Polymer 134 (2018) 155–162

Contents lists available at ScienceDirect

Polymer

journal homepage: www.elsevier.com/locate/polymer

Surface-modified cellulose nanocrystals for biobased epoxy nanocomposites

Liang Yue [a], Anthony Maiorana [b], Farid Khelifa [c], Ammar Patel [a], Jean-Marie Raquez [c], Leïla Bonnaud [c], Richard Gross [b], Philippe Dubois [c], Ica Manas-Zloczower [a, *]

[a] Department of Macromolecular Science and Engineering, Case Western Reserve University, 2100 Adelbert Road, Kent Hale Smith Bldg, Cleveland, OH, 44106, USA
[b] New York State Center for Polymer Synthesis, Department of Chemistry and Chemical Biology, Rensselaer Polytechnic Institute, 110 8th Street, Troy, N.Y, 12180, USA
[c] Laboratory of Polymeric and Composite Materials, Center of Innovation and Research in Materials and Polymers (CIRMAP), Materia Nova Research Center and University of Mons, Place du Parc 23, 7000, Mons, Belgium

ARTICLE INFO

Article history:
Received 23 September 2017
Received in revised form
17 November 2017
Accepted 22 November 2017
Available online 22 November 2017

Keywords:
Biobased epoxy resin
Nanocomposite
Cellulose nanocrystal
Surface modification
Dispersion

ABSTRACT

Herein a unique strategy for cellulose nanocrystal functionalization is presented in the form of surface functionalization of cellulose nanocrystals. Cellulose nanocrystals were prepared from acid hydrolysis of ramie fibers and then further subjected to amine functionalization with an amino trimethoxy silane (APTMS). The introduction of surface amine functionality to the cellulose nanocrystal allowed for an additional reaction with a biobased epoxy resin derived from diphenolic acid. The resulting thermo-mechanical properties of epoxy nanocomposites with amine functionalized cellulose nanocrystal were on average more than 7 times improved. Specifically, the storage modulus at 160 °C increased from 19.5 MPa for the neat resin to 151.5 MPa for the composite with 10 wt% APTMS modified CNC. The results reported herein demonstrate that amine functionalized cellulose nanocrystals provide excellent dispersion in epoxy resin systems and are a viable route to utilization of both biobased nanofillers and biobased epoxy resins.

1. Introduction

Epoxy resins are among the most versatile thermoset polymers available and are used in a wide range of applications. They represent the matrix of choice for high strength composites, corrosion resistant coatings, structural adhesives and electronic materials. Wind turbine blades, printed circuit boards, and structural adhesives used in automobile assembly all utilize epoxy resins primarily due to their high glass transition temperature, elastic modulus, toughness, and adjustable viscosity [1].

In the epoxy industry, Bisphenol A and Novolacs represent benchmark materials due to their ability to impart desired physical and thermal properties in cured resins. Bisphenol A has recently come under extensive criticism due to its potential to disrupt the endocrine system [2–4]. Novolacs are manufactured from phenol/formaldehyde and can contain high amounts of Bisphenol F. Furthermore, both bisphenol A and novolacs are primarily derived from petroleum feedstocks and are ultimately unsustainable.

Recent advances in biobased epoxy resins have yielded an extensive array of sustainable platform chemicals that could provide a route to petroleum feedstock replacement. Most notable of the biobased epoxy resin platforms are epoxidized vegetable oils that are already used as ingredients for protective coatings [5,6]. Other platforms are epoxidized tree rosins, diglycidyl ethers and esters of furans, cashew nutshell liquid based epoxy resins, multifunctional glycidyl flavonoids, diglycidyl ferulates, and diglycidyl diphenolates [7–13].

One challenge in utilizing biobased resins is that their inherent structure can lead to decreases in final polymer properties such as glass transition temperature and modulus [10,14–17]. Often, the performance of biobased resins is not benchmarked against current commercial systems that leads to a lack of information on their potential for commercialization [18]. Recently, advances in high modulus nanofillers such as graphene, carbon nanotubes, and silica have shown promise in producing materials that exceed the thermal and physical properties of the neat thermoset matrix [19].

* Corresponding author.
E-mail address: ixm@case.edu (I. Manas-Zloczower).

https://doi.org/10.1016/j.polymer.2017.11.051
0032-3861/

However, the industrial adoption of these fillers is relatively difficult due to production costs, inherent dangers associated with their use, and difficulty in obtaining good dispersions due to surface chemistry.

Cellulose nanocrystals (CNCs), extracted from abundant cellulose, represent a nanofiller that is sustainable, biodegradable, and has excellent strength-to-weight ratio, and can be used as reinforcement for epoxy composites [20,21]. In order to fully realize the potential performance of CNCs as nano-building blocks in polymeric systems, it is important to modify the hydroxyl rich CNC surface in order to achieve filler separation and individualization within hydrophobic matrices. Extensive attention has been given to CNC modification methodologies such as grafting hydrophobic polymers from and to their surface. Modification techniques often utilize reactions of CNC hydroxyl groups to perform esterification, silanization, and epoxide ring opening [22–24].

In the absence of suitable catalysts and reaction conditions, the nucleophilicity of CNC hydroxyl groups is low. Consequently, ring-opening of epoxide groups by CNC hydroxyl moieties proceeds slowly. In contrast, primary aliphatic amines are much better nucleophiles for epoxy ring-opening reactions. Recently, Dubois and coworkers reported the silanization of CNC surfaces to introduce a wide variety of functional groups. This led to the improved dispersion of these modified CNCs in polylactide [25]. Indeed, organosilanization chemistry offers a mild method that can be carried out under aqueous conditions without protection-deprotection chemistry, and that enables the introduction of primary amines to CNC surfaces.

We hypothesized that amine functionalization of CNC through the use of amino-silanes would allow for ring-opening of epoxy groups during their dispersion in epoxy resins. Such ring-opening reactions will result in CNC surface chemistry that is identical to the matrix and will lead to well-dispersed CNC-epoxy nanocomposites. This dispersion method would also avoid the use of organic solvents. Based on earlier work on CNC epoxy thermoset nanocomposites, we further hypothesized that good dispersion of modified CNCs will lead to improvements in nano-reinforced composite thermomechanical properties at lower nanofiber loading than had previously been reported [26].

Herein we report the preparation of amine modified CNC utilizing 3-(aminopropyl)trimethoxysilane (APTMS). CNC surface modification was assessed through spectroscopic techniques including X-ray Photoelectron Spectroscopy (XPS) and Fourier Transform Infrared (FTIR). Amine functionalized CNCs at various concentrations were dispersed in a biobased epoxy derived from diphenolic acid and the dispersion quality was assessed through rheological and microscopic techniques. The amine functionalized CNC showed improved dispersion and better mechanical and thermal properties in the cured nanocomposites relative to unmodified CNC epoxy composites. To further support the choice of APTMS, other silane-modifications with 3-(trimethoxysilyl)propyl methacrylate (MPS), diethoxy(3-glycidyloxypropyl)methylsilane (GPTMS) and trimethoxy(propyl)silane (PTMO) were performed following the same procedure and their dispersion performance was also studied.

2. Experimental

2.1. Materials

Biobased epoxy resin DGEDP-ethyl (diglycidyl ether of diphenolate ethyl ester) was synthesized as previously reported [27]. 3-Aminopropyltrimethoxysilane (APTMS), 3-(Trimethoxysilyl)propyl methacrylate (MPS), Diethoxy(3-glycidyloxypropyl) methylsilane (GPTMS) and Trimethoxy(propyl)silane (PTMO) and isophorone diamine (IPDA) were purchased from Sigma-Aldrich. Pure ramie fibers obtained from Stucken Melchers GmbH & Co. (Germany). All chemicals were used as received.

2.2. Preparation of cellulose nanocrystals (CNC)

CNCs were extracted from ramie fibers as described in a previous paper [26]. In summary, 80 g purified ramie fibers were cut into small pieces and treated with 1 L of 4% NaOH solution at 80 °C for 2 h to remove any residual hemicellulose or lignin. These fibers were then acid hydrolyzed in 800 mL sulfuric acid solution (65 wt %) at 55 °C for 30 min under continuous mechanical stirring. The obtained suspension was thoroughly washed with water until neutrality, dialyzed against deionized water for a few days and then filtered through a sintered glass to remove non-hydrolyzed fibers. Dry CNCs were recovered by freeze-drying.

2.3. Organosilanization of CNC

APTMS (100 mM) was dissolved in an ethanol/water mixture (80/20 w/w, 100 mL) and the solution pH was maintained at about 4 with a citrate buffer (10 mM). This solution was maintained at ambient temperature with magnetic stirring for 2 h [28,29]. CNCs (0.5 g) were then added to this solution and the mixture was maintained at ambient temperature with magnetic stirring for an additional 2 h. The APTMS grafted CNCs were washed with water by centrifugation and recovered as a solid residue after freeze-drying. Subsequently, the APTMS grafted CNCs were maintained at 110 °C for 16 h under vacuum.

2.4. Preparation of CNC/epoxy composites

APTMS modified CNCs were dispersed in the biobased epoxy resin (DGEDP-ethyl) at concentrations of 1, 5 and 10 wt% by ultrasonication (10 g batch, 2 min at 60 °C, 10s on/off pause mode with an amplitude of 45%). Equimolar ratio of IPDA was added and well mixed. This mixture was centrifuged to remove trapped air and then transferred to Teflon coated stainless steel molds at room temperature till gelling occurs. The samples were further cured under compression molding at constant pressure (2 T) for 4 h at 80 °C and then another 4 h at 160 °C. Composites with unmodified CNCs were prepared following an identical method as described above.

2.5. Characterizations

2.5.1. Infrared spectroscopy

Fourier transform infrared (FTIR) measurements were performed using a Bruker Tensor 17 spectrometer in the range from 500 to 4000 cm^{-1}.

2.5.2. XRD

XRD were conducted using a Siemens D 5000 with Cu Kα radiation in the range of $2\theta = 5–30°$.

2.5.3. TEM

TEM images of CNC particles were taken with a Philips CM200 with an acceleration voltage of 20 kV.

2.5.4. XPS

XPS analysis was performed with an Axis Ultra spectrometer (Kratos Analytical). The X-ray source was used under standard conditions with an operating pressure of 10^{-8} Torr.

2.5.5. Optical microscopy

After sonication, CNC/epoxy suspensions were observed with a Leica DMRXP optical microscope in transmission mode. Images were taken with a QImaging QICAM digital camera under polarized light.

2.5.6. Differential scanning calorimetry (DSC)

DSC measurements were conducted with a DSC Q100 from TA Instruments with T_{zero} aluminum pans. Each sample was ramped from 0 to 250 °C at a heating rate of 5 °C/min under nitrogen.

2.5.7. Thermogravimetric analysis (TGA)

TGA measurements were conducted with a TGA Q500 from TA Instruments with aluminum pans. Samples were heated at 10 °C/min under nitrogen flow.

2.5.8. Dynamic mechanical analysis (DMA)

Mechanical behaviors were analyzed with a Q800 DMTA from TA Instruments in tensile mode with a constant frequency of 1 Hz, strain amplitude of 0.05% and in a temperature range of 20–180 °C.

2.5.9. Rheology

Rheological properties of CNC/epoxy suspensions were obtained at 25 °C on a TA Instruments ARES G2 rheometer with 25 mm parallel plate geometry and a 1 mm gap size. Frequency sweeps from 0.1 to 100 rad/s at strain level of 0.1% were conducted within the linear viscoelastic regime.

3. Results and discussion

3.1. Organosilanization of CNC

Modification of CNCs by salinization is believed to occur as follows. In the presence of excess ethanol, and pH values about 4, silane hydrolysis occurs [29]. Due to the large amount of free hydroxyl groups on CNC surfaces, silanols form stable hydrogen bonds with the CNCs. Annealing under vacuum at 110 °C promotes further condensation and formation of a well-defined polysiloxane layer onto the CNC surface (see Scheme S1) [28,30,31].

Primary amine groups of APTMS modified CNCs are observed by FTIR (Fig. 1). For unmodified CNC, the broad peak ranging from 3024 cm^{-1} to 3691 cm^{-1} is due to CNC free O-H stretching vibrations. For APTMS modified CNC, the primary amine N-H stretch that occurs from 3300 cm^{-1} to 3500 cm^{-1} is overlapped with O-H stretching vibrations. The N-H in-plane-bend vibrational bands with both peaks at 1560 cm^{-1} and 1640 cm^{-1} also indicate the presence of primary amine groups on APTMS modified CNC (CNC-APTMS), comparing the only peak at 1640 cm^{-1} for unmodified CNC which comes from stretch of C=C bonding [25,32]. The formation of Si-O-C and Si-O-Si by condensation of the hydroxyl groups were not easily observed, due to the strong cellulose C-O-C vibration (1050-1170 cm^{-1}) [30].

XPS analysis in Fig. 2 shows the presence of a N_{1s} peak for the APTMS modified CNC, which was not observed for non-modified CNCs. Table 1 lists changes in the elements after modification and an increase of Si amount supports APTMS grafting to CNCs. The surface O/C ratio of APTMS modified and non-modified CNCs is 0.69 and 0.79, respectively. This decrease in the O/C ratio upon APTMS modification is due to the carbon-richer (propyl moiety of APTMS).

FTIR and XPS analyses highlight the presence of primary amine groups onto the CNC. Furthermore, the thermal stability of CNCs increased by APTMS modification (T_d-onset from 287 °C to 352 °C, see Figure S6) due to the formation of a dense polysiloxane layer on CNC surfaces which delays thermal decomposition.

TEM images (Fig. 3) display individual CNC nanoparticles for both modified and pristine CNC samples. Unmodified CNC shows typical dimensions for CNC extracted from ramie fibers (length ~250 nm, diameter ~10 nm) as previously reported. [25]The average diameter of the APTMS modified CNC (~25 nm) is slightly higher than those of unmodified CNC. This morphological change of CNC-APTMS is attributed to the formation of a polysiloxane layer on CNC surface. Indeed, similar results have been reported for other silane modified CNCs [25].

The impact of silanization on CNC crystallinity was evaluated by XRD. The diffraction profiles of unmodified and modified CNCs are shown in Fig. 3 (bottom). The XRD curve of unmodified CNCs is typical of a cellulose type 1 pattern, with characteristic diffraction peaks at 15° and 22° on the 2θ scale. The XRD patterns show both crystalline and amorphous regions in the form of diffraction bands and a diffuse pattern. The XRD patterns for unmodified and CNC-APTMS are similar, indicating that the crystalline structure of the CNC is not affected by surface modification. Crystallinity degree calculated from Segal equation ($I_c=(I_{22.6}-I_{18})/I_{22.6}$) are 78.3% for CNC and 78.1% for CNC-APTMS [33].

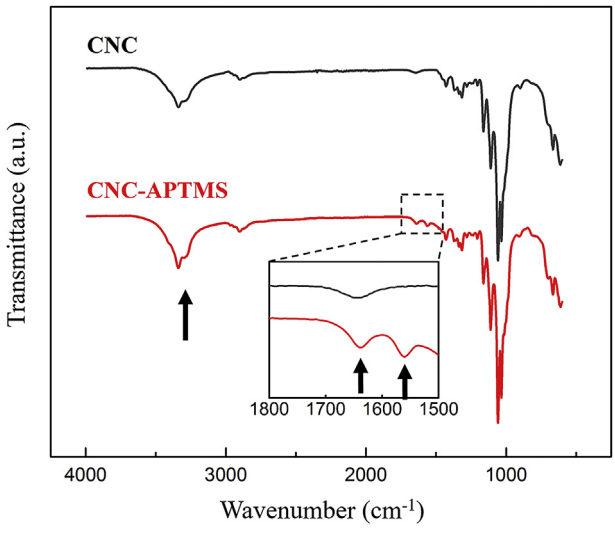

Fig. 1. FTIR of non-modified and APTMS modified CNCs.

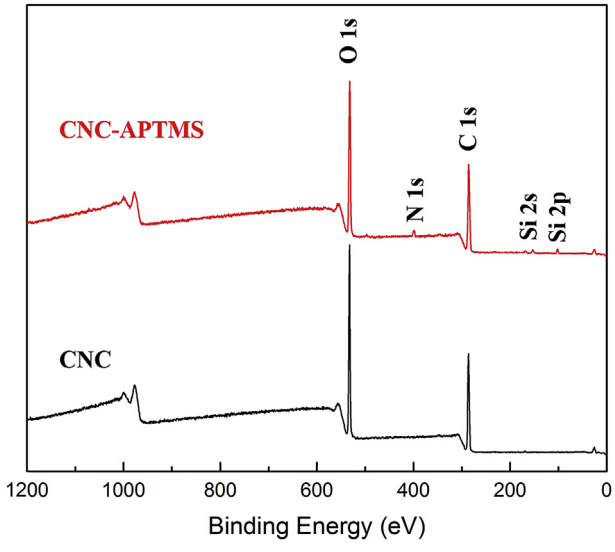

Fig. 2. XPS spectra of CNC and APTMS modified CNC.

Table 1
Atomic percentage of elements for CNC and APTMS modified CNC from XPS.

	C (at. %)	O (at. %)	Si (at. %)	N (at. %)
CNC	55.7	44.3	0	0
CNC-APTMS	57.1	39.4	1.8	1.6

3.2. CNC/epoxy composites

The dispersion state of CNCs in the biobased epoxy resin after mixing by ultrasonication, but before curing, was evaluated with optical microscopy. The anisotropic CNC crystalline structure can be distinguished from the isotropic epoxy resin under polarized light in transmission mode [32]. Therefore, observation of large birefringent domains would indicate CNC aggregation. Fig. 4 shows micrographs of suspensions after sonication at different concentrations. For unmodified CNC/epoxy suspensions at all concentrations, birefringent domains on the order of 100 μm are observed, indicating that unmodified CNCs form large aggregates in the epoxy matrix. In contrast, APTMS modified CNCs show little aggregation with almost no birefringent domains in the micrographs at any of the concentrations studied. Since mixing by ultrasonication of epoxy resin and CNC-APTMS resulted in an exotherm that was evident by an increase in dispersion temperature, we believe that some fraction of APTMS-modified CNCs react with DEGDP-ethyl epoxy groups enabling better dispersion within the matrix. In contrast, unmodified CNCs having only hydroxyl groups which are not sufficiently nucleophilic to react with DEGDP-ethyl will form aggregates within the matrix as observed by optical microscopy.

The CNC dispersion state in biobased epoxy resin was also investigated by performing frequency sweep rheological measurements. The dependence of complex viscosity (η^*) and storage modulus (G') on the oscillatory frequency (ω) are shown in Fig. 5. For the neat biobased epoxy monomer, the complex viscosity remains constant through a wide range of frequencies, indicative of Newtonian behavior. For dispersions containing unmodified CNCs, the complex viscosity follows a similar trend as that of the neat epoxy resin with relatively small increases at 5 and 10 wt% filler. In contrast, CNC-APTMS dispersions show a significantly different behavior with pronounced shear thinning. The storage modulus for dispersions containing 5 and 10 wt% CNC-APTMS display solid-like behavior with a plateau region at low frequencies. This is indicative of filler network formation as a result of good dispersion. In the case of unmodified CNC dispersions, solid-like behavior is not observed at all concentrations, highlighting the absence of a filler network and a lack of good particle dispersion. The slight decrease in viscosity from around 49 to 47 Pa s for the 1 wt % unmodified CNC sample is within the instrument error.

Besides the APTMS modified CNC, we have also modified CNC with the MPS, GPTMS and PTMO to render them more hydrophobic. Results for the biobased epoxy resin with different modified CNC are presented in the Supporting Information. Among all the modified CNC, the CNC-APTMS show the best results for dispersion quality. Consequently, the properties of the CNC-APTMS/epoxy composites were further investigated.

The glass transition temperature (T_g) of the biobased epoxy

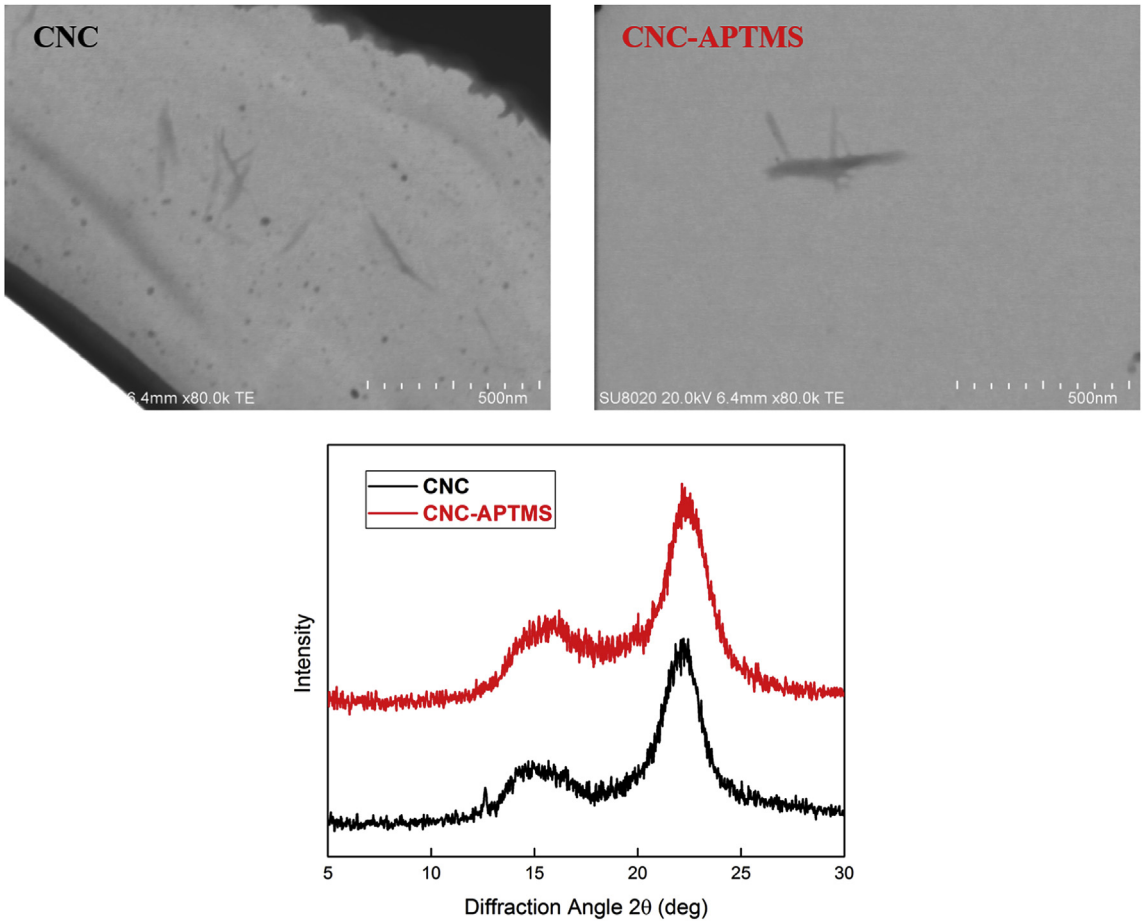

Fig. 3. TEM images (top) and XRD patterns (bottom) of CNC and APTMS modified CNC particles.

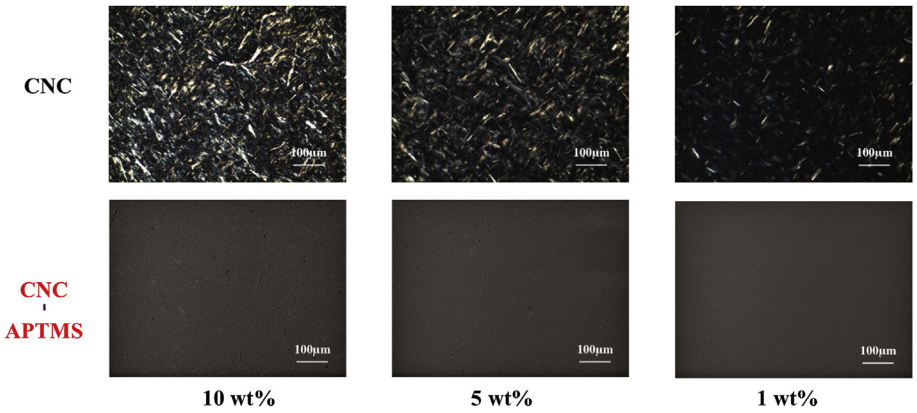

Fig. 4. Images from optical microscopy under polarized light of biobased epoxy resin/CNC dispersions formed after mixing by ultrasonication, but before curing.

composites after curing was studied by DSC. Fig. 6 displays first-heat DSC traces of neat biobased epoxy and epoxy/CNC nanocomposites with various CNC contents. No significant exothermic peaks were observed on heating which indicates that all samples were cured to the maximum degree of conversion before testing. The T_g value was determined by the midpoint of the drop observed in the heat flow versus temperature curve. T_g of the neat epoxy is 126.4 °C, while that of nanocomposites increased with CNC loading.

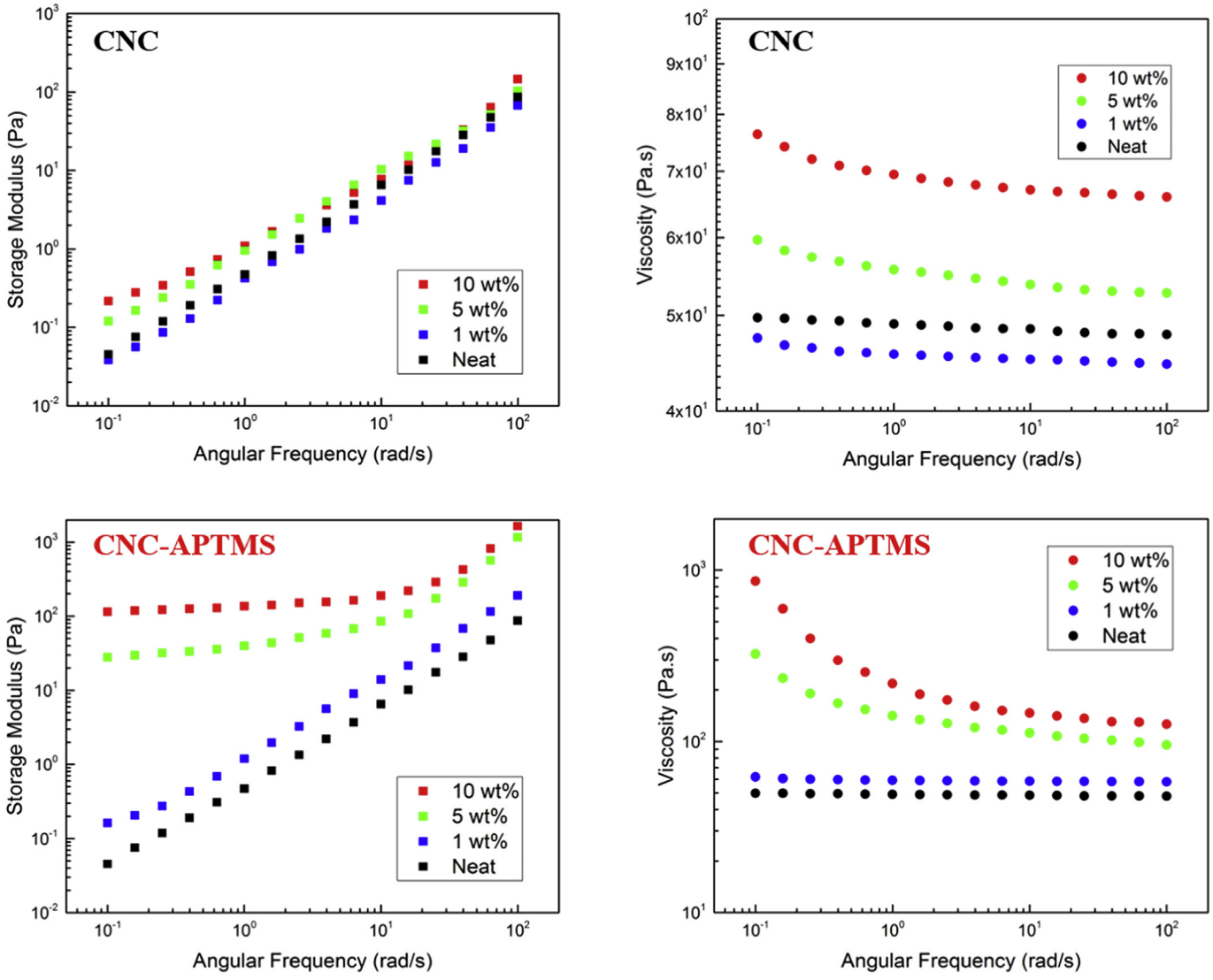

Fig. 5. Storage modulus and complex viscosity as function of frequency of biobased epoxy resin/CNC dispersions formed after mixing by ultrasonication, but before curing.

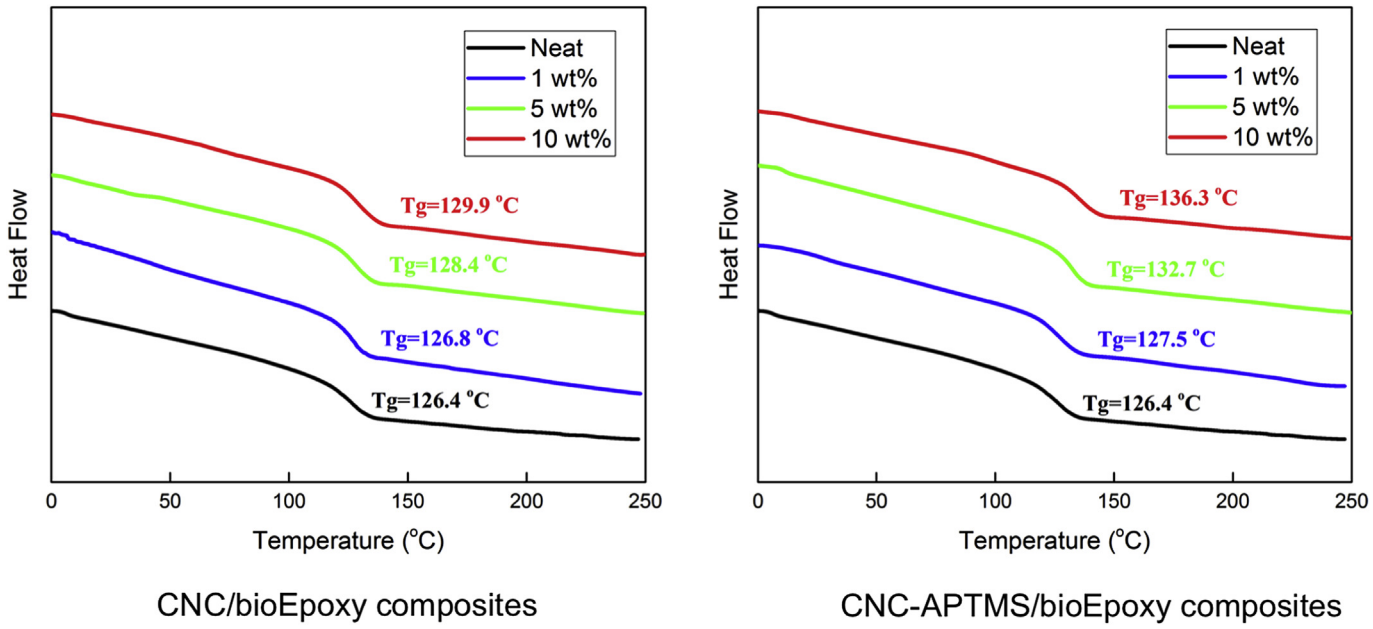

Fig. 6. DSC curves of cured CNC and APTMS modified CNC epoxy composites and Tg.

For unmodified CNC composites, small increases in T_g were observed for samples loaded with 1 and 5 wt% of CNC, while the T_g increased by 3.5 °C at 10 wt% CNC. The CNC-APTMS epoxy composites display relatively larger increases in T_g, especially at 5 and 10 wt% (6.3 and 9.9 °C, respectively). The effect of nanofillers on epoxy resin T_g is attributed to a reduction in polymer chain mobility [19]. It is believed that CNCs act as physical interlocking points in the cured matrix restraining chain mobility [34]. For unmodified CNCs, nanoparticle agglomeration limits this "restriction effect". The ability of APTMS-modified CNC surface primary amine moieties to react with DEGDP-ethyl epoxy groups resulting in stronger interfacial interactions between the nanofiller and matrix creating additional barriers that restrict chain motion and cause T_g to shift to higher temperatures.

The thermo-mechanical properties of the biobased epoxy nanocomposites were investigated by DMA and Fig. 7 shows the storage modulus and alpha transition temperatures (tan δ, associated to T_g) of the nanocomposites. The neat resin and nanocomposites both show typical amorphous thermoset behavior: below T_g the storage modules decreases slightly with increasing temperature and above T_g the storage modulus rapidly drops. Both unmodified and APTMS modified CNC nanocomposites display higher storage modulus. Below T_g, the increase in storage modulus for the nanocomposites at the same filler loading was similar for the unmodified and APTMS modified CNCs. However, above T_g, the storage modulus of CNC-APTMS nanocomposites was significantly higher than for the unmodified CNC nanocomposites. For example, at 160 °C, the storage modulus of 10 wt% APTMS modified CNCs nanocomposite is 151.5 MPa, more than 7 times larger compared to the neat resin (19.5 MPa), whereas, with 10 wt% unmodified CNCs,

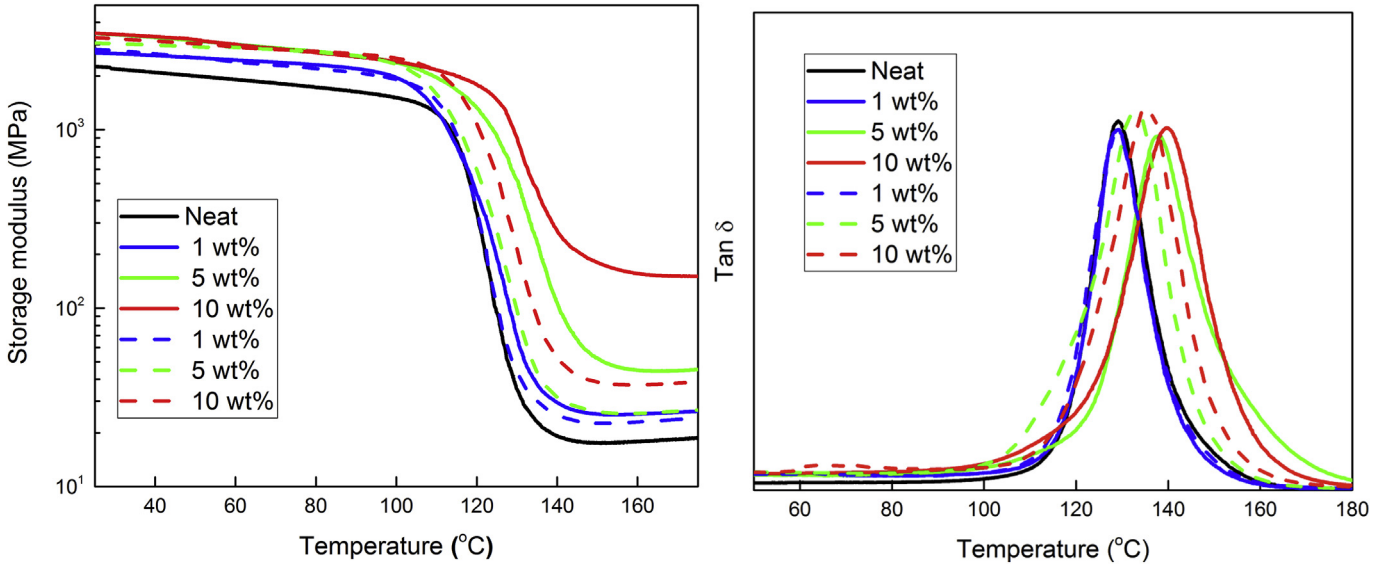

Fig. 7. Storage modulus and tan(δ) as a function of temperature of the epoxy composites. Unmodified CNCs are shown by dashed lines and APTMS modified CNCs are shown as solid lines.

Table 2
T_g from DMA and DSC in addition to the storage modulus at 25 °C and 160 °C for the unmodified and APTMS-modified CNC/epoxy composites.

Samples		Tg from DMA °C	Tg from DSC °C	Storage modulus at 25 °C MPa	Storage modulus at 160 °C MPa
Neat DGEDP-ethyl		129.2	126.4	2405 ± 68	19.5 ± 3.6
CNC-APTMS	1 wt	129.4	127.5	2765 ± 55	25.8 ± 2.9
	5 wt	137.9	132.7	3265 ± 63	44.4 ± 5.5
	10 wt	139.8	136.3	3492 ± 72	151.5 ± 37.4
Unmodified CNC	1 wt	129	128.4	2786 ± 64	23.5 ± 3.2
	5 wt	133.2	126.8	2915 ± 86	26.1 ± 4.5
	10 wt	135.2	129.9	3309 ± 82	37.3 ± 5.9

the storage modulus was only 37.3 MPa. The significant reinforcement of CNC-APTMS nanocomposites above T_g is attributed to the well dispersed rigid nanofiller in the matrix. Also, considering the presence of amine functional groups on modified CNCs, a potential reaction between filler and the biobased epoxy could also facilitate the reinforcement. Glass transition temperatures from tan δ curves show the same trend as that from DSC. A comparison of T_g values from DMA and DSC is shown in Table 2, along with the tensile storage modulus at 25 °C and 160 °C for all samples. These results further confirm the strong interactions between APTMS-CNCs and the biobased DGEDP-ethyl resin.

Besides, the thermal stability of the composites was studied with TGA (See S7). The thermal stability of the composites increased compare to the neat biobased epoxy. Similar results have been reported previously, as the CNC content increased, the temperature at the maximum weight loss rate of the composites shift to higher temperature [32,35].

4. Conclusions

Free hydroxyl groups at the surface of CNCs derived from ramie fibers were modified by silanization with APTMS. XPS analysis provided definitive evidence that APTMS modification resulted in CNC fiber surfaces decorated with amines. Improved dispersion quality of CNC-APTMS relative to unmodified CNCs was evident from optical micrographs obtained under polarized light for the biobased epoxy resin/CNCs dispersions before curing. Furthermore, increases in T_g for 5 and 10% loaded CNC-APTMS nanocomposites were substantially higher than for the systems containing unmodified CNCs. This provides further evidence that APTMS modification of CNCs enables physical interlocking points in the cured matrix restraining chain mobility. The improved dispersion of CNC-APTMS is attributed to the reaction of amino groups with DGEDP-ethyl epoxy groups increasing compatibility between filler and matrix components. In addition, rheology measurements demonstrate that the storage modulus for dispersions containing 5 and 10 wt% CNC-APTMS display solid-like behavior with a plateau region at low frequencies, indicative of filler network formation. Good dispersion of the CNC-APTMS as well as stronger filler-matrix interactions contributes to the significant improvement in storage modulus above T_g.

Acknowledgements

The authors are grateful for funding received from the National Science Foundation Partnerships for International Research and Education (PIRE) Program (Award #1243313). The research in Mons is supported by the Science Policy Office of the Belgian Federal Government (PAI 7/5), the European Commission/Walloon Region (FEDER – BIORGEL, MACOBIO RF projects – Valicell – INTERREG V BIOCOMPAL), and by the Belgian National Fund for Scientific Research (FNRS). J.M.R. is a FNRS research fellow.

Appendix A. Supplementary data

Supplementary data related to this article can be found at https://doi.org/10.1016/j.polymer.2017.11.051.

References

[1] R. Auvergne, S. Caillol, G. David, B. Boutevin, J.-P. Pascault, Biobased thermosetting epoxy: present and future, Chem. Rev. 114 (2) (2014) 1082–1115.
[2] M.V. Maffini, B.S. Rubin, C. Sonnenschein, A.M. Soto, Endocrine disruptors and reproductive health: the case of bisphenol-A, Mol. Cell. Endocrinol. 254–255 (2006) 179–186.
[3] M.-Y. Chen, M. Ike, M. Fujita, Acute toxicity, mutagenicity, and estrogenicity of bisphenol-A and other bisphenols, Environ. Toxicol. 17 (1) (2002) 80–86.
[4] J.C. O'Connor, R.E. Chapin, Critical evaluation of observed adverse effects of endocrine active substances on reproduction and development, the immune system, and the nervous system, Pure Appl. Chem. 75 (11–12) (2003) 2099–2123.
[5] M. Stemmelen, F. Pessel, V. Lapinte, S. Caillol, J.-P. Habas, J.-J. Robin, A fully biobased epoxy resin from vegetable oils: from the synthesis of the precursors by thiol-ene reaction to the study of the final material, J. Polym. Sci. Part A Polym. Chem. 49 (11) (2011) 2434.
[6] A. Patel, A. Maiorana, L. Yue, R.A. Gross, I. Manas-Zloczower, Curing kinetics of biobased epoxies for tailored applications, Macromolecules 49 (15) (2016) 5315–5324.
[7] A.-L. Brocas, A. Llevot, C. Mantzaridis, G. Cendejas, R. Auvergne, S. Caillol, S. Carlotti, H. Cramail, Epoxidized rosin acids as co-precursors for epoxy resins, Des. Monomers Polym. 17 (4) (2014) 301–310.
[8] M. Sultania, J.S.P. Rai, D. Srivastava, Process modeling, optimization and analysis of esterification reaction of cashew nut shell liquid (CNSL)-derived epoxy resin using response surface methodology, J. Hazard. Mater. 185 (2–3) (2011) 1198–1204.
[9] M. Janvier, L. Hollande, A.S. Jaufurally, M. Pernes, R. Ménard, M. Grimaldi, J. Beaugrand, P. Balaguer, P.-H. Ducrot, F. Allais, Syringaresinol: a renewable and safer alternative to bisphenol a for epoxy-amine resins, ChemSusChem 10 (4) (2017) 738–746.
[10] E.D. Hernandez, A.W. Bassett, J.M. Sadler, J.J. La Scala, J.F. Stanzione, Synthesis and characterization of bio-based epoxy resins derived from vanillyl alcohol, ACS Sustain. Chem. Eng. 4 (8) (2016) 4328–4339.
[11] A. Llevot, E. Grau, S. Carlotti, S. Grelier, H. Cramail, Selective laccase-catalyzed dimerization of phenolic compounds derived from lignin: towards original symmetrical bio-based (bis) aromatic monomers, J. Mol. Catal. B Enzym. 125 (2016) 34–41.
[12] A. Maiorana, A.F. Reano, R. Centore, M. Grimaldi, P. Balaguer, F. Allais, R.A. Gross, Structure property relationships of biobased n-alkyl bisferulate epoxy resins, Green Chem. 18 (18) (2016) 4961–4973.
[13] R. Ménard, S. Caillol, F. Allais, Ferulic acid-based renewable esters and amides-containing epoxy thermosets from wheat bran and beetroot pulp: chemo-enzymatic synthesis and thermo-mechanical properties characterization, Ind. Crops Prod. 95 (2017) 83–95.
[14] A. Maiorana, L. Yue, I. Manas-Zloczower, R. Gross, Structure–property relationships of a bio-based reactive diluent in a bio-based epoxy resin, J. Appl. Polym. Sci. 133 (2016) 43635.
[15] A. Kadam, M. Pawar, O. Yemul, V. Thamke, K. Kodam, Biodegradable biobased epoxy resin from karanja oil, Polymer 72 (2015) 82–92.
[16] R. Liu, X. Zhang, S. Gao, X. Liu, Z. Wang, J. Yan, Bio-based epoxy-anhydride thermosets from six-armed linoleic acid-derived epoxy resin, RSC Adv. 6 (58) (2016) 52549–52555.
[17] M.D. Garrison, B.G. Harvey, Bio-based hydrophobic epoxy-amine networks derived from renewable terpenoids, J. Appl. Polym. Sci. 133 (45) (2016).
[18] E.A. Baroncini, S. Kumar Yadav, G.R. Palmese, J.F. Stanzione, Recent advances in bio-based epoxy resins and bio-based epoxy curing agents, J. Appl. Polym. Sci. 133 (45) (2016).
[19] L. Yue, G. Pircheraghi, S.A. Monemian, I. Manas-Zloczower, Epoxy composites with carbon nanotubes and graphene nanoplatelets – dispersion and synergy effects, Carbon 78 (2014) 268–278.
[20] L. Tang, C. Weder, Cellulose whisker/epoxy resin nanocomposites, ACS Appl. Mater. Interfaces 2 (4) (2010) 1073–1080.

[21] S.X. Peng, S. Shrestha, Y. Yoo, J.P. Youngblood, Enhanced dispersion and properties of a two-component epoxy nanocomposite using surface modified cellulose nanocrystals, Polymer 112 (2017) 359–368.
[22] M. Singh, A. Kaushik, D. Ahuja, Surface functionalization of nanofibrillated cellulose extracted from wheat straw: effect of process parameters, Carbohydr. Polym. 150 (2016) 48–56.
[23] W. Hu, S. Chen, J. Yang, Z. Li, H. Wang, Functionalized bacterial cellulose derivatives and nanocomposites, Carbohydr. Polym. 101 (2014) 1043–1060.
[24] H.-Y. Yu, Z.-Y. Qin, C.-F. Yan, J.-M. Yao, Green nanocomposites based on functionalized cellulose nanocrystals: a study on the relationship between interfacial interaction and property enhancement, ACS Sustain. Chem. Eng. 2 (4) (2014) 875–886.
[25] J.-M. Raquez, Y. Murena, A.-L. Goffin, Y. Habibi, B. Ruelle, F. DeBuyl, P. Dubois, Surface-modification of cellulose nanowhiskers and their use as nano-reinforcers into polylactide: a sustainably-integrated approach, Compos. Sci. Technol. 72 (5) (2012) 544–549.
[26] F. Khelifa, Y. Habibi, L. Bonnaud, P. Dubois, Epoxy monomers cured by high cellulosic nanocrystal loading, ACS Appl. Mater. Interfaces 8 (16) (2016) 10535–10544.
[27] A. Maiorana, S. Spinella, R.A. Gross, Bio-based alternative to the diglycidyl ether of bisphenol A with controlled materials properties, Biomacromolecules 16 (3) (2015) 1021–1031.
[28] A.S. Singha, A.K. Rana, Effect of aminopropyltriethoxysilane (APS) treatment on properties of mercerized lignocellulosic grewia optiva fiber, J. Polym. Environ. 21 (1) (2012) 141–150.
[29] M. Abdelmouleh, S. Boufi, A. ben Salah, M.N. Belgacem, A. Gandini, Interaction of silane coupling agents with cellulose, Langmuir 18 (8) (2002) 3203–3208.
[30] S.C.M. Fernandes, P. Sadocco, A. Alonso-Varona, T. Palomares, A. Eceiza, A.J.D. Silvestre, I. Mondragon, C.S.R. Freire, Bioinspired antimicrobial and biocompatible bacterial cellulose membranes obtained by surface functionalization with aminoalkyl groups, ACS Appl. Mater. Interfaces 5 (8) (2013) 3290–3297.
[31] M.-C.B. Salon, G. Gerbaud, M. Abdelmouleh, C. Bruzzese, S. Boufi, M.N. Belgacem, Studies of interactions between silane coupling agents and cellulose fibers with liquid and solid-state NMR, Magn. Reson. Chem. 45 (6) (2007) 473–483.
[32] S. Xu, N. Girouard, G. Schueneman, M.L. Shofner, J.C. Meredith, Mechanical and thermal properties of waterborne epoxy composites containing cellulose nanocrystals, Polymer 54 (24) (2013) 6589–6598.
[33] L.Y. Mwaikambo, M.P. Ansell, Chemical modification of hemp, sisal, jute, and kapok fibers by alkalization, J. Appl. Polym. Sci. 84 (12) (2002) 2222–2234.
[34] K.L. Pickering, M.G.A. Efendy, T.M. Le, A review of recent developments in natural fibre composites and their mechanical performance, Compos. Part A Appl. Sci. Manuf. 83 (2016) 98–112.
[35] N. Saba, A. Safwan, M. Sanyang, F. Mohammad, M. Pervaiz, M. Jawaid, O. Alothman, M. Sain, Thermal and Dynamic Mechanical Properties of Cellulose Nanofibers Reinforced Epoxy Composites, vol. 102, 2017.